

Statistical Forecasts for the Occurrence of Precipitation Outperform Global Models over Northern Tropical Africa

Peter Vogel¹, Peter Knippertz¹, Tilmann Gneiting², Andreas H. Fink¹, Manuel Klar³, and Andreas Schlueter⁴

¹Karlsruhe Institute of Technology

²Heidelberg Institute for Theoretical Studies; Karlsruhe Institute of Technology

³Trier University

⁴Stanford University

November 21, 2022

Abstract

Short-term global ensemble predictions of rainfall currently have no skill over northern tropical Africa when compared to simple climatology-based forecasts, even after sophisticated statistical postprocessing. Here we demonstrate that statistical forecasts for the probability of precipitation based on a simple logistic regression model have considerable potential for improvement. The new approach we present here relies on gridded rainfall estimates from the Tropical Rainfall Measuring Mission for July–September 1998–2017 and uses rainfall amounts from the pixels that show highest positive and negative correlations on the previous two days as input. Forecasts using this model are reliable and have a higher resolution and better skill than climatology-based forecasts. The good performance is related to westward propagating African easterly waves and embedded mesoscale convective systems. The statistical model is outmatched by the postprocessed dynamical forecast in the dry outer tropics only, where extratropical influences are important.

1 **Statistical Forecasts for the Occurrence of Precipitation**
2 **Outperform Global Models over Northern Tropical**
3 **Africa**

4 **Peter Vogel^{1,2}, Peter Knippertz¹, Tilmann Gneiting^{2,3}, Andreas H. Fink¹,**
5 **Manuel Klar^{3*}, and Andreas Schlueter^{1†}**

6 ¹Institute of Meteorology and Climate Research, Karlsruhe Institute of Technology, Germany

7 ²Heidelberg Institute for Theoretical Studies, Heidelberg, Germany

8 ³Institute for Stochastics, Karlsruhe Institute of Technology, Germany

9 **Key Points:**

- 10 • Raw and statistically postprocessed global ensembles fail to predict West African
11 rainfall occurrence.
12 • A logistic regression model using observations from preceding days outperforms
13 all other forecasts.
14 • The skill is mainly related to propagating African easterly waves and mesoscale
15 convective systems.

*currently at Department of Mathematics, Trier University, Trier, Germany

†currently at Department of Computer Science, Stanford University, Stanford, California, USA

Corresponding author: Peter Knippertz, peter.knippertz@kit.edu

Abstract

Short-term global ensemble predictions of rainfall currently have no skill over northern tropical Africa when compared to simple climatology-based forecasts, even after sophisticated statistical postprocessing. Here we demonstrate that statistical forecasts for the probability of precipitation based on a simple logistic regression model have considerable potential for improvement. The new approach we present here relies on gridded rainfall estimates from the Tropical Rainfall Measuring Mission for July–September 1998–2017 and uses rainfall amounts from the pixels that show highest positive and negative correlations on the previous two days as input. Forecasts using this model are reliable and have a higher resolution and better skill than climatology-based forecasts. The good performance is related to westward propagating African easterly waves and embedded mesoscale convective systems. The statistical model is outmatched by the postprocessed dynamical forecast in the dry outer tropics only, where extratropical influences are important.

Plain Language Summary

Forecasts of precipitation for the next few days based on state-of-the-art weather models are currently inaccurate over northern tropical Africa, even after systematic forecast errors are corrected statistically. In this paper, we show that we can use rainfall observations from the previous two days to improve predictions of precipitation occurrence. Such an approach works well over this region, as rainfall systems tend to travel from east to west organized by flow patterns several kilometers above the ground, called African easterly waves. This statistical forecast model requires training over a longer time period (here 19 years) to establish robust relationships on which future predictions can be based. The input data employed are gridded rainfall estimates based on satellite data for the African summer monsoon in July to September. The new method outperforms all other methods currently available on a day-to-day basis over the region, except for the dry outer tropics, where influences from midlatitudes, which are better captured by weather models, become more important.

1 Introduction

Large parts of tropical Africa depend on rain-fed agriculture (Wani et al., 2009). Accurate precipitation forecasts on the 1–5-day timescale could help improve many aspects of the farmers’ day-to-day work such as ploughing, planting, (usually small-scale) irrigation, harvest, and livestock management. Other areas that would benefit from improved rainfall information include hydropower energy production, water resource management, disease and flood prevention as well as road safety. Arguably such information are currently much more valuable practically than decadal or climate projections (Singh et al., 2018).

A recent paper by Vogel et al. (2018) investigated the skill of nine global ensemble prediction systems participating in TIGGE (Bougeault et al., 2010) to forecast precipitation over northern tropical Africa during the extended summer monsoon season (01 May to 15 October) 2007–2014. The model forecasts were compared against a so-called extended probabilistic climatology (EPC), essentially an ensemble prediction constructed from past observations for a given calendar day along with a 2-day window around that date. It was found that raw ensemble forecasts from all nine models (and the multi-model ensemble) are uncalibrated and unreliable, and underperform in the prediction of occurrence and amount of precipitation when compared to EPC. This assessment holds for the three investigated subregions West and East Sahel and Guinea Coast, and is robust against accumulation periods from 1 to 5 days and grid spacings from $0.25^\circ \times 0.25^\circ$ to $2^\circ \times 5^\circ$. Consistent results were found for the satellite-based Tropical Rainfall Measur-

65 ing Mission (TRMM) 3B42 gridded product and raingauge data from the Karlsruhe African
66 Surface Station Database (KASS-D).

67 To improve the model forecasts, the two state-of-the-art statistical postprocessing
68 methods Ensemble Model Output Statistics (EMOS) (Gneiting et al., 2005; Scheuerer,
69 2014) and Bayesian Model Averaging (BMA) (Raftery et al., 2005; Sloughter et al., 2007)
70 were applied by Vogel et al. (2018). Both consistently improve the forecasts' calibration
71 and reliability but the overall predictive performance is hardly better than that of EPC.
72 Only the multi-model ensemble shows slightly positive skill for all eight investigated years.
73 Vogel et al. (2018) speculate that this sobering result is related to the fact that the con-
74 vective parametrizations used in global models struggle to realistically represent mesoscale
75 convective systems (MCSs), which largely dominate the rainfall generation in the region
76 (Mathon et al., 2002; Fink et al., 2006; Maranan et al., 2018). This deficit has been shown
77 to also deteriorate larger-scale circulations on timescales of five days and more in numer-
78 ical weather prediction models (Marsham et al., 2013; Pante & Knippertz, 2019). An ex-
79 tension of the analysis by Vogel et al. (2018) to the entire tropical belt from 30°S and
80 30°N (Vogel et al., manuscript to be submitted to *Weather and Forecasting*) shows that
81 tropical Africa stands out to have the lowest predictive skill – even after postprocess-
82 ing – of all tropical continents. This result holds for rainfall occurrence, amount, and ex-
83 tremes at accumulation periods of 1 to 5 days. The fact that this region is exceptional
84 in its degree of convective organization (Nesbitt et al., 2006; Roca et al., 2014) supports
85 its potential role in forecast degradation (Vogel et al., 2018).

86 While the results summarized above are disappointing and require further inves-
87 tigation, they also call for the development of alternative approaches. Various studies
88 have shown that rainfall over tropical Africa is by no means as erratic as the low model
89 skill suggests, but is in fact modulated on the synoptic to planetary scale by tropical wave
90 phenomena, most prominently African easterly waves (AEWs) (Schlueter, Fink, Knip-
91 pertz, & Vogel, 2019). The dominant influence of AEWs on precipitation over West Africa
92 has been known for several decades (Reed et al., 1977; Mekonnen et al., 2006; Lavaysse
93 et al., 2006). According to Fink and Reiner (2003), more than 60% of MCSs in West Africa
94 are associated with AEWs. The combination of quasi-linear waves that influence the oc-
95 currence and propagation of long-lived MCSs via modulations of lower tropospheric shear,
96 midlevel relative humidity, and convective available potential energy (CAPE) (Schlueter,
97 Fink, & Knippertz, 2019) points to potential forecast improvements through statistical
98 models based on spatio-temporal correlation patterns in observations. Such models may
99 outperform dynamical models, as these struggle to represent the coupling between con-
100 vection and tropical waves (Elless & Torn, 2018; Dias et al., 2018) and at the same time
101 display higher sharpness and resolution than EPC due to knowledge of the current at-
102 mospheric situation. To test this hypothesis, here we present results for a probabilistic
103 forecast model for precipitation occurrence over northern tropical Africa based on a sim-
104 ple logistic regression approach. Statistical forecast methods were more common at times
105 when computational power was more limited, but the concept has largely been abandoned
106 as numerical weather prediction has become increasingly skillful in the extratropics (Wilks,
107 2019, Section 7.9.1). A famous example of a statistical forecast is the so-called "Yester-
108 day" method that is based on observations from preceding days and was used in trop-
109 ical Africa in the mid 20th century (Schove, 1946). However, we are unaware of any re-
110 cent study of statistical approaches to (synoptic) rainfall forecasting in Africa.

111 The following Section 2 gives an overview of the employed data and methods. In
112 Section 3 the spatio-temporal correlation of precipitation is analyzed, forming the ba-
113 sis for a statistical forecast method and its evaluation in Section 4. Finally, Section 5 presents
114 the main conclusions and an outlook.

2 Data and methods

Our study is based on the TRMM 3B42-V7 gridded product (Huffman et al., 2007) that is used for the creation of an EPC, for forecast validation, and the development of statistical forecasts. TRMM merges active measurements from the precipitation radar with passive, radar-calibrated information from infrared as well as microwave measurements. The precipitation estimates are calibrated against nearby gauge observations on a monthly basis. The TRMM data are available on a $0.25^\circ \times 0.25^\circ$ grid with 3-hourly temporal resolution but were accumulated here to daily sums and to $1^\circ \times 1^\circ$ gridboxes. The spatial aggregation, however, had little impact on the obtained spatio-temporal correlations (not shown). The investigations are focused on the core summer monsoon season (July–September) for the 20 years from 1998–2017. The study region is northern tropical Africa from 25°W – 50°E and 3 – 18°N (corresponding to the area shown in Fig. 4). All investigations are made for the probability of precipitation (PoP), for which we set a threshold of 0.2 mm per day. The satellite-based rainfall data are used to construct an EPC forecast with a ± 2 -day window as in Vogel et al. (2018).

For comparison, we include corresponding forecasts from the Integrated Forecasting System of the European Centre for Medium-Range Weather Forecasts (ECMWF) for the years since 2011, subsequent to a major increase in the resolution of the model grid. See <https://www.ecmwf.int/en/publications/ifs-documentation> for a comprehensive documentation. Data were downloaded on the standard reduced Gaussian grid and then regridded with the Climate Data Operator (CDO) software to $1^\circ \times 1^\circ$ to match the TRMM data. As Vogel et al. (2018) showed substantial improvement when applying statistical postprocessing to the raw ensemble forecasts, we include here also ECMWF forecasts postprocessed using the EMOS method consistent with their results.

The statistical forecast will follow a simple strategy. For each TRMM gridbox, we analyze the relationship between 1-day accumulated precipitation at the location considered, and rainfall amounts at just any gridbox one and two days before, using Spearman’s rank correlation. This allow us to identify the locations with the strongest statistical relationships (both in a positive and negative sense), which we then use to construct the statistical model. Specifically, let o_1^+ , o_2^+ , o_1^- , and o_2^- denote the observations at lags of one and two days at the strongest positively and negatively correlated gridboxes, respectively. We employ a logistic regression model of the form

$$\text{logit}(p) \mid o_1^+, o_2^+, o_1^-, o_2^-, d = a_1^+ f(o_1^+) + a_2^+ f(o_2^+) + a_1^- f(o_1^-) + a_2^- f(o_2^-) + s(d), \quad (1)$$

for the forecast probability p , where $\text{logit}(p) = \log(p/(1-p))$. The function $f(x) = \log(x+0.001)$ transforms a nonnegative precipitation amount to the real line, and the term

$$s(d) = b_0 + b_1 \sin(2\pi d/365) + b_2 \cos(2\pi d/365) \quad (2)$$

depends on the day of the year d in a periodic fashion. To train such a model one needs to distinguish between verification and training data. When issuing predictions for a July–September period in a given year, observations from that year are used for verification, while observations from all other years from within 1998–2017 are used for training. So altogether, the following steps are conducted for each gridbox: We (a) find Spearman’s rank correlations from the training data to identify the locations with the highest positive and negative correlation coefficients at lags of one and two days, (b) estimate the parameters a_1^+ , a_2^+ , a_1^- , a_2^- , b_0 , b_1 , and b_2 of the statistical model in Eqs. 1 and 2 with the iteratively reweighted least squares technique, and (c) compute PoP forecasts for each day of the verification period based on the values of o_1^+ , o_2^+ , o_1^- , o_2^- , and d at hand.

For EMOS, we follow common practice, use a rolling training period of the most recent 500 days, comprising data from both the gridbox at hand and the eight neighboring gridboxes, provided they share the respective land/water characteristic, and apply the estimation methods described by Scheuerer (2014) and Vogel et al. (2018). So ul-

166 timately, four different types of PoP forecasts are generated and compared in this pa-
 167 per: a climatological prediction (termed EPC), raw model ensemble output (ENS), a post-
 168 processed model prediction (EMOS), and a purely statistical forecast (Logistic).

169 **3 Spatio-temporal correlation of precipitation**

170 To illustrate the statistical forecast method, an example application is discussed
 171 here for Niamey. In Figure 1 the panels at left show Spearman’s rank correlation results
 172 for July–September 1998–2017. At a lag of a single day, precipitation at Niamey is most
 173 strongly correlated (above the 99th percentile of the correlation coefficients in the study
 174 region) with an east–west extended, spatially coherent region along the eastern part of
 175 the border between Niger and Nigeria. The pixel with the highest value overall, which
 176 is used in the logistic regression model, is located at 13.5°N and 10.5°E and thus almost
 177 exactly 8 degrees (ca. 900 km) to the east of Niamey. This propagation speed is slightly
 178 faster than that of a typical AEW of 9.1 ms⁻¹ (ca. 800 km per day) but considerably
 179 slower than that of a typical MCS of 15 ms⁻¹ (ca. 1300 km per day) (Fink & Reiner,
 180 2003). The corresponding analysis for a lag of two days shows a further shift of the area
 181 of highest correlation upstream to a maximum located at 14.5°N and 19.5°E, correspond-
 182 ing to a distance of about 1000 km and thus in good agreement with the behavior on
 183 the previous day. The correlation values are lower but the extremal region remains spa-
 184 tially coherent. Overall, this supports our assumption that information on recent rain-
 185 fall events propagates with MCSs and AEWs. The fact that the relationship is robust
 186 over two days points to a key role of AEW propagation for convection, as MCSs typi-
 187 cally have shorter lifetimes of around 12h (Fink & Reiner, 2003).

188 In contrast, the strongest negative correlations are found to the south of Niamey
 189 for both lags. For the first day, the region is fairly coherent and stretches from south-
 190 western Ghana to southeastern Burkina Faso, culminating in northern Togo. For the sec-
 191 ond day, there is much less spatial coherence and the most extreme value occurs over north-
 192 western Nigeria and thus much closer to Niamey than for the positive correlations. The
 193 interpretation of the negative correlation results is less clear. It is conceivable that they
 194 also reflect AEW influence on precipitation indicating suppression in the downstream
 195 ridge. Knippertz et al. (2017) documented regional north–south fluctuations in rainfall
 196 associated with propagating disturbances during the DACCIWA campaign in June–July
 197 2016. Another possibility is a north–south shift in the monsoonal rainfall belt as discussed
 198 on subseasonal (Janicot et al., 2011) and interannual (Nicholson, 2008) time scales.

199 The center and right-hand side panels in Figure 1 illustrate the modulation of the
 200 PoP at Niamey conditional on the accumulated precipitation amounts at the highest posi-
 201 tively correlated locations at lags of one and two days (denoted o_1^+ and o_2^+ in Eq. 1).
 202 We categorize these precipitation amounts into no, light, and strong rainfall. The top
 203 center panel displays the PoP at Niamey conditional on the categorical precipitation at
 204 lag one day. From an average climatological value of 0.50 (marked by black lines), the
 205 PoP reduces to 0.42 for no precipitation at a lag of one day at the location marked with
 206 a cross in the top left panel and increases to 0.71 if strong precipitation occurred there.
 207 For a lag of two days (bottom right panel), the range of deviations from climatology de-
 208 creases only slightly with values of 0.44 and 0.68, respectively. Considering both obser-
 209 vations jointly (bottom center panel) reveals even stronger modulations of the PoP. If
 210 at both lags no precipitation was observed at the respective locations, the PoP at Ni-
 211 amey falls to 0.37, while it is 0.81, thus more than double, for strong precipitation on
 212 both previous days. This clearly illustrates the potential in our approach.

213 **4 Statistical forecasts for the occurrence of precipitation**

214 Based on the correlation results discussed in the previous section, Figure 2 displays
 215 a July–September 2016 time series of logistic regression-based forecasts for Niamey (Lo-

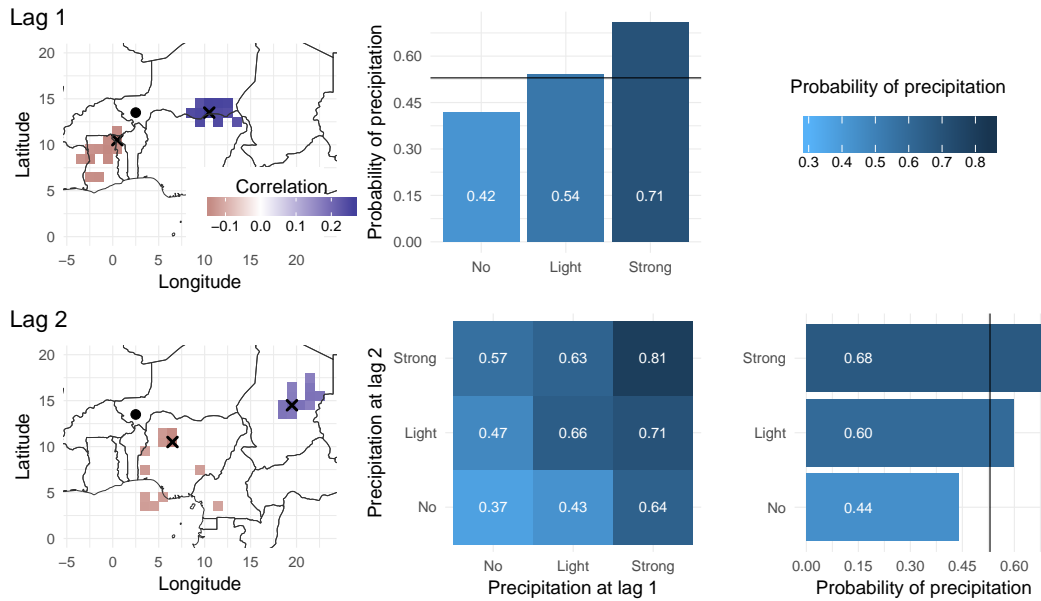


Figure 1. Spatio-temporal correlation of precipitation for the gridbox of Niamey (black dot). Displayed are the strongest 1% of positive (blue) and negative (red) correlations between 1-day accumulated precipitation at Niamey and surrounding gridboxes at lags of one (top left) and two (bottom left) days, based on Spearman’s rank correlation and the period July–September 1998–2017, with the locations of the highest and lowest values overall indicated by crosses. The center bottom panel shows the PoP at Niamey conditional on both 1- and 2-day lagged categorized precipitation values, while the neighboring panels show the corresponding marginally conditioned probabilities. The black lines mark the climatological PoP of 0.50. The categories of light and strong rainfall are separated by the climatological median of the non-zero precipitation amounts.

216 gistic, blue line) in comparison with the direct ECMWF model output (ENS, black dots),
 217 postprocessed ECMWF predictions (EMOS, orange line), and the climatology-based fore-
 218 cast (EPC, red line). The actual observed rainfall occurrence is marked with grey shad-
 219 ing.

220 The EPC forecast reflects the average annual cycle with PoP increasing from 0.50
 221 at the beginning of July to a maximum of about 0.67 in mid-August and a fall-off to 0.30
 222 at the end of September, which is associated with the advance and retreat of the West
 223 African monsoon. Observations in 2016 roughly correspond with this seasonal evolution
 224 showing frequent rainfall with longer wet periods in mid-July and mid-August, and a ten-
 225 dency towards drier conditions in September. The ENS forecast reveals an obvious ten-
 226 dency to forecast rainfall occurrence with certainty (i.e., with probability 1.00), while
 227 lower PoPs are generally rare. EMOS postprocessing changes this dramatically to a PoP
 228 prediction that follows the seasonal cycle reflected in EPC, while taking into account the
 229 tendencies for drier or wetter conditions evident in ENS. Finally Logistic shares many
 230 of the characteristics evident in EMOS but varies more strongly from about 0.20 to 0.80.
 231 This indicates an overall better resolution of Logistic.

232 The procedure demonstrated in Figures 1 and 2 was repeated for all other years
 233 of our comparison period July–September 2011–2017. Figure 3 shows the resulting reli-
 234 ability diagrams, where the observed relative frequency is plotted versus the forecast
 235 probability in 10% bins (blue lines). The inset histograms indicate the number of cases
 236 in the bins. The ENS forecast confirms the impression from Figure 2 that the raw en-

Niamey (Niger) July – September 2016

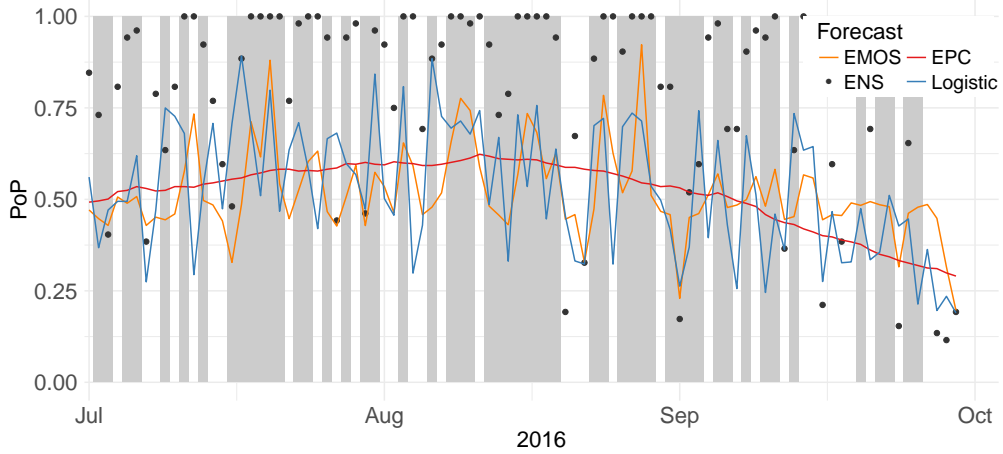


Figure 2. ENS (black dots), EMOS (orange line), EPC (red line), and Logistic (blue line) forecasts for the occurrence of precipitation at the gridpoint of Niamey (marked with a dot in the left panels of Figure 1) during July–September 2016, and the actual occurrence of precipitation indicated by grey shading. For a description of the different forecast types, see Section 2.

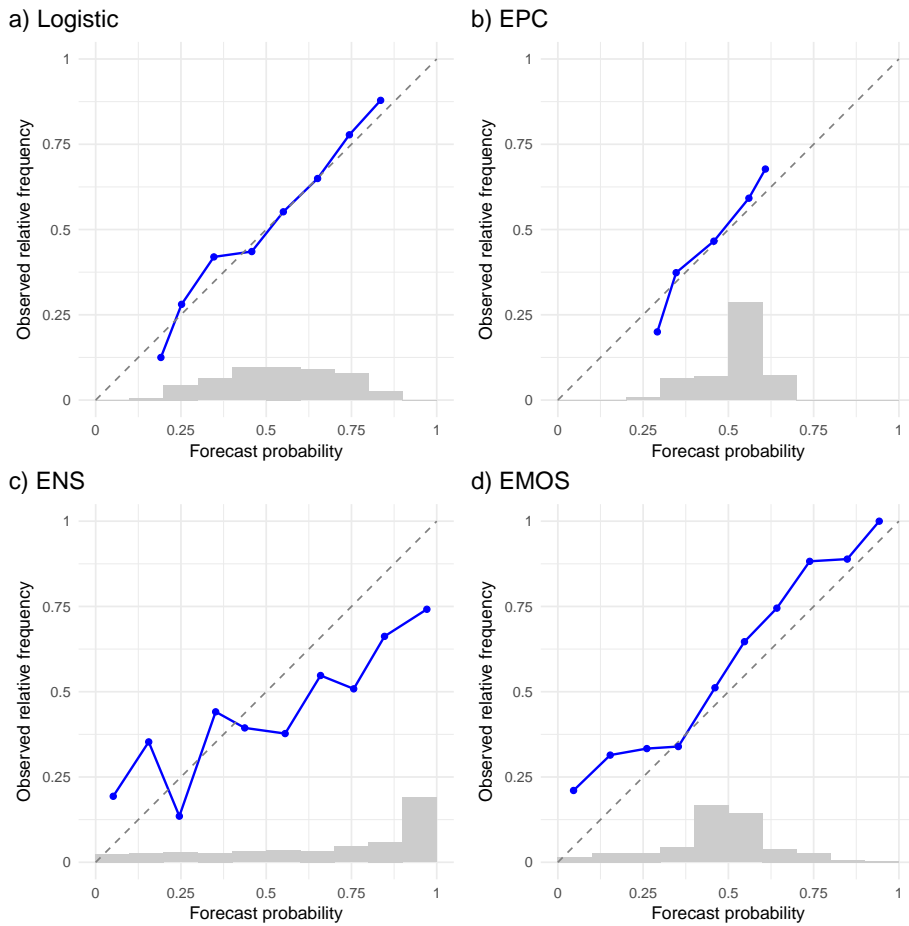
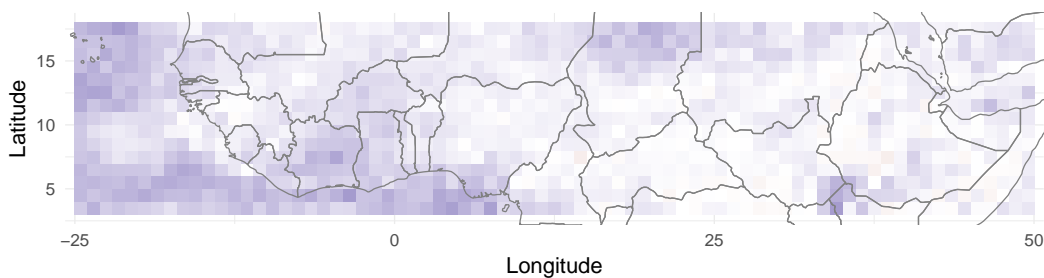


Figure 3. Reliability diagrams for a) Logistic, b) EPC, c) ENS, and d) EMOS forecasts of PoP at the gridpoint of Niamey for July–September 2011–2017.

a) Logistic vs. EPC



b) Logistic vs. EMOS

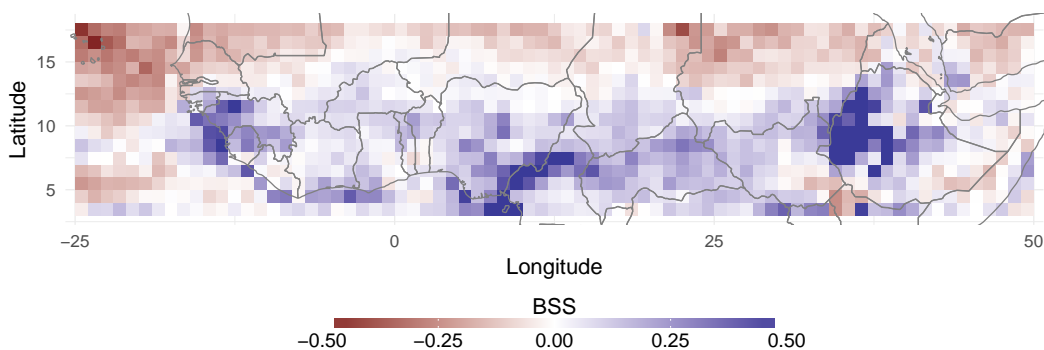


Figure 4. Spatial display of the Brier skill score (BSS) for Logistic relative to a) EPC and b) EMOS forecasts for July–September 2011–2017.

237 semble frequently predicts rain with certainty, which however only verifies in about 75%
 238 of the respective cases (Figure 3, panel c). The other forecast probability bins are rel-
 239 atively uniformly populated, hinting at good resolution. However, the reliability of ENS
 240 is unsatisfactory with overall too wet conditions for dry forecasts and vice versa. EPC
 241 displays much better reliability but low resolution with forecast probabilities only vary-
 242 ing between 0.25 and 0.65. The EMOS forecast clearly combines elements of EPC and
 243 ENS (panels b–d). Despite the noisiness inherited from ENS, reliability is much improved,
 244 while resolution is reduced through the influence of climatological information. Finally,
 245 the Logistic forecast (panel a) clearly shows the most superior forecasts with reliability
 246 similar to EPC but much higher resolution.

247 In order to gauge the predictive performance of the Logistic forecast on the regional
 248 scale, we extend the approach exemplified above for Niamey to all gridboxes in the study
 249 region for July–September 2011–2017. Panel a in Figure 4 displays the spatial distribu-
 250 tion of the Brier skill score (BSS) of the Logistic forecast relative to EPC. It shows that
 251 skill increases – or stays the same – over all of northern tropical Africa and the adjacent
 252 tropical Atlantic Ocean. The spatial average of the BSS amounts to 0.061, with values
 253 for individual gridboxes ranging from -0.039 to 0.239 . There is no obvious geograph-
 254 ical pattern to the improvement, apart perhaps from a slight tendency for higher val-
 255 ues in the west where AEWs are usually more intense and couple more strongly to or-
 256 ganized convection (Fink & Reiner, 2003). Land-ocean contrasts may also play a role.

257 Panel b shows the BSS relative to EMOS. Here a much clearer geographical pat-
 258 tern emerges. Improvements are pronounced over terrestrial areas to the south of about
 259 13°N , while the northern Sahel and southern Sahara as well as oceanic areas mostly show

260 a degradation of the forecast. Our example gridbox at Niamey is located close to the bor-
 261 der between these areas, where forecast improvement by Logistic over EMOS is neutral.
 262 The spatial average is still positive at 0.038 but reduced compared to the BSS relative
 263 to EPC. This pattern suggests that Logistic outperforms EMOS where AEWs have a strong
 264 influence on daily rainfall (Schlueter, Fink, Knippertz, & Vogel, 2019), a connection that
 265 is known to be ill represented in dynamical models (Marsham et al., 2013; Pante & Knip-
 266 pertz, 2019). An additional factor appears to be problems with orographic precipitation
 267 in the ECMWF model, as Logistic is particularly superior over all major mountain ar-
 268 eas of the southern zone, i.e., the Ethiopian Highlands, the Cameroon Line Mountains,
 269 and the Guinea Highlands in the far west. In these areas the BSS reaches values of more
 270 than 0.50, even though one would expect orographic effects to be systematic enough to
 271 be corrected for by postprocessing. This result therefore requires a more in-depth anal-
 272 ysis, which is beyond the scope of this paper.

273 The relatively poor performance in the dry region to the north suggests that the
 274 occasional rainfalls in this area are not primarily caused by meridionally propagating waves
 275 that have been shown to lose their influence to the north of 15°N (Schlueter, Fink, Knip-
 276 pertz, & Vogel, 2019). Past case studies suggest that here precipitation is often associ-
 277 ated with anomalous influences from the extratropics (Cuesta et al., 2010; Roehrig et
 278 al., 2011; Vizy & Cook, 2014) and it is plausible that these are better represented by a
 279 dynamical model due to their rather episodic nature. At locations near the extratrop-
 280 ical boundary of our study region, propagating signals from the north cannot be repre-
 281 sented by the statistical model. It is interesting to note that the good performance of
 282 EMOS is most pronounced over the ocean around the Cape Verde Islands, a region that
 283 is known to be affected by upper-level troughs from the midlatitudes, even occasionally
 284 in the summer half year (Fröhlich & Knippertz, 2008).

285 These results demonstrate that no single method alone can resolve the problem of
 286 poor dynamical model performance over northern tropical Africa and that future work
 287 should try attempting to blend dynamical and statistical information in an optimal way.

288 5 Conclusions

289 Motivated by the poor performance of dynamical forecast models to predict rain-
 290 fall over northern tropical Africa, we have demonstrated that it is possible to construct
 291 skillful statistical forecasts for precipitation occurrence on the basis of information about
 292 recent rainfall events alone. The method we have developed uses gridded precipitation
 293 data from TRMM for the period July–September 1998–2017. For a given location and
 294 day, we first identify pixels with the strongest positive and negative correlations on the
 295 previous days from a training dataset. Rainfall amounts at these locations and times have
 296 then be employed to train a logistic regression model for rainfall occurrence at the tar-
 297 get location and time. This model is ultimately used to make forecasts for a verification
 298 period. The predictions obtained this way are then compared to a probabilistic forecast
 299 based on climatology (EPC) as well as raw and postprocessed ensemble predictions from
 300 the ECMWF. The main conclusions from this analysis are:

- 301 • The statistical forecasts are reliable and have higher resolution than climatology-
 302 based forecasts, as they take the current weather situation into account.
- 303 • They outperform EPC forecasts over most of northern tropical Africa and the ad-
 304 jacent Atlantic Ocean with an area-mean BSS of 0.06.
- 305 • Exemplary correlation patterns and the geographical distribution of forecast skill
 306 of the statistical model suggest that westward propagation of AEWs and MCSs,
 307 possibly together with synoptic-scale latitudinal shifts in the monsoon system, are
 308 underlying reasons for the good performance.
- 309 • Over areas where precipitation is more sporadic and more strongly influenced by
 310 the usually more predictable extratropical circulation, such as the northern Sa-

311 hel/southern Sahara and the adjacent Atlantic Ocean, the statistical model is out-
 312 performed by postprocessed ensemble predictions based on the ECMWF model.

313 To our knowledge, the results presented are the first-ever demonstration of success-
 314 ful short-term statistical rainfall forecasts over the region and we advocate that such ap-
 315 proaches be considered as an attractive alternative to the widely distributed direct model
 316 output. It should be noted, however, that such a model (in particular such a simple one)
 317 can only work if there is a strong and consistent physical mode that dominates rainfall
 318 variability. In other regions where rainfall is more chaotic and/or several wave modes
 319 superimpose, our approach will likely not be as powerful as over West Africa. Neverthe-
 320 less, this initial success provides strong motivation to expand the concept to (a) precip-
 321 itation amounts, (b) other tropical regions, (c) longer leadtimes, (d) other rainfall datasets
 322 (particularly as TRMM is not active anymore), (e) more sophisticated statistical tech-
 323 niques (in particular convolutional neural networks that allow exploiting the full spatio-
 324 temporal correlation pattern, possibly even including interactions of different wave types),
 325 and (f) additional input data (e.g., moisture or wind variables). This can ultimately help
 326 to meet the large challenge to create a hybrid forecast system that combines the strengths
 327 of dynamical models, postprocessing, and statistical forecasting in an optimal way.

328 Acknowledgments

329 The research leading to these results has been accomplished within project C2 “Pre-
 330 diction of wet and dry periods of the West African Monsoon” of the Transregional Col-
 331 laborative Research Center SFB/TRR 165 “Waves to Weather” funded by the German
 332 Science Foundation (DFG). TG is grateful for support by the Klaus Tschira Foundation.
 333 TRMM data are available at <https://pmm.nasa.gov/data-access/downloads/trmm>.
 334 ECMWF forecast data are available at <https://www.ecmwf.int/en/forecasts/datasets>.

335 References

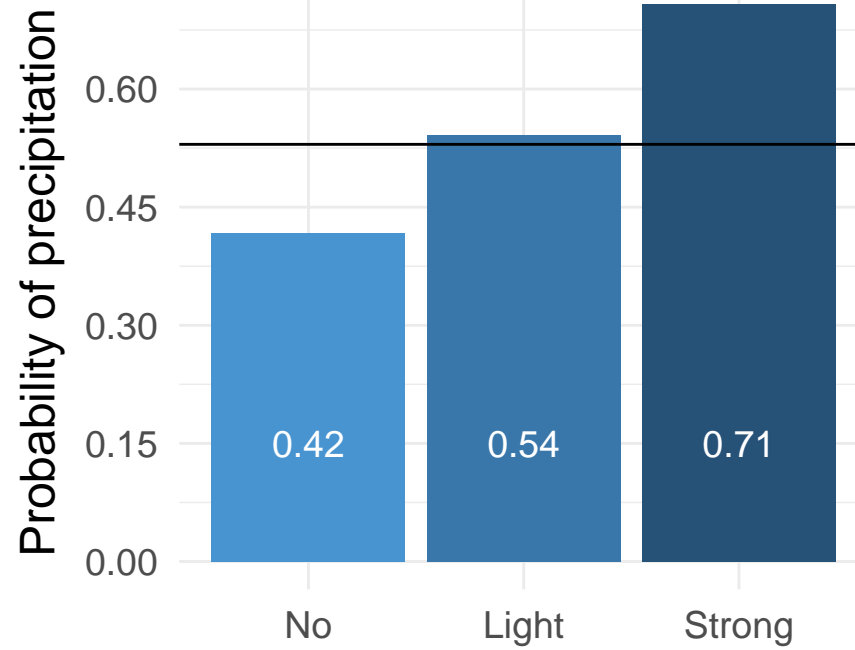
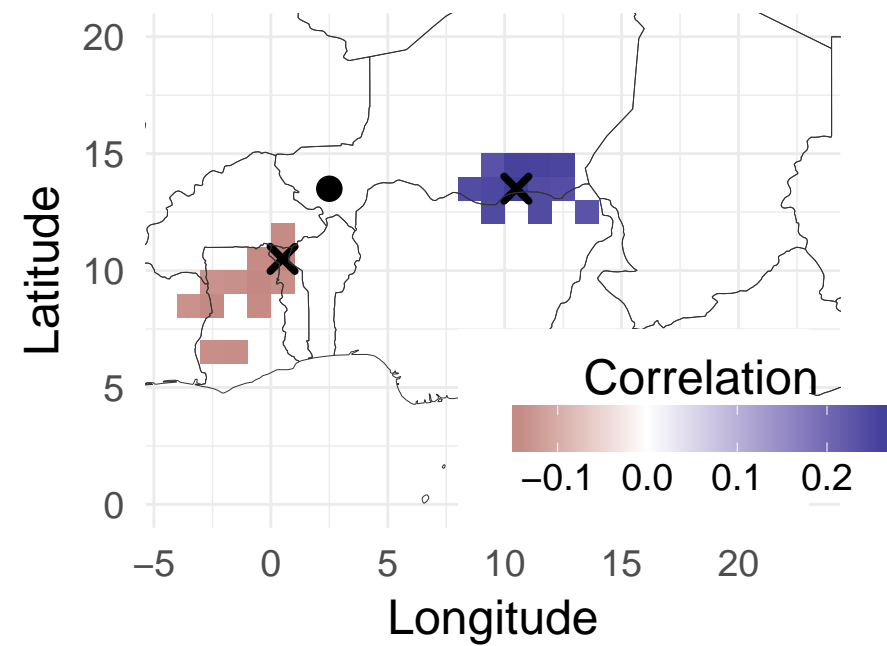
- 336 Bougeault, P., Toth, Z., Bishop, C., Brown, B., Burridge, D., Chen, D. H., ... Wor-
 337 ley, S. (2010). The THORPEX interactive grand global ensemble. *Bull. Amer.*
 338 *Meteorol. Soc.*, *91*(8), 1059–1072. doi: 10.1175/2010BAMS2853.1
- 339 Cuesta, J., Lavaysse, C., Flamant, C., Mimouni, M., & Knippertz, P. (2010). North-
 340 ward bursts of the West African monsoon leading to rainfall over the Hog-
 341 gar Massif, Algeria. *Quart. J. Roy. Meteorol. Soc.*, *136*(s1), 174–189. doi:
 342 10.1002/qj.439
- 343 Dias, J., Gehne, M., Kiladis, G. N., Sakaeda, N., Bechtold, P., & Haiden, T.
 344 (2018). Equatorial waves and the skill of NCEP and ECMWF numeri-
 345 cal weather prediction systems. *Mon. Wea. Rev.*, *146*(6), 1763–1784. doi:
 346 10.1175/MWR-D-17-0362.1
- 347 Elless, T. J., & Torn, R. D. (2018). African Easterly Wave forecast verification
 348 and its relation to convective errors within the ECMWF ensemble prediction
 349 system. *Wea. Forecasting*, *33*(2), 461–477. doi: 10.1175/WAF-D-17-0130.1
- 350 Fink, A., & Reiner, A. (2003). Spatiotemporal variability of the relation between
 351 African easterly waves and West African squall lines in 1998 and 1999. *J. Geo-*
 352 *phys. Res.*, *108*, 4332. doi: 10.1029/2002JD002816
- 353 Fink, A., Vincent, D., & Ermert, V. (2006). Rainfall types in the West African Su-
 354 danian zone during the summer monsoon 2002. *Mon. Wea. Rev.*, *134*, 2143–
 355 2164. doi: 10.1175/MWR3182.1
- 356 Fröhlich, L., & Knippertz, P. (2008). Identification and global climatology of upper-
 357 level troughs at low latitudes. *Meteorol. Zeitschrift*, *17*(5), 565–573. doi: 10
 358 .1127/0941-2948/2008/0320
- 359 Gneiting, T., Raftery, A. E., Westveld, A. H., & Goldman, T. (2005). Cal-
 360 ibrated probabilistic forecasting using ensemble model output statistics

- 361 and minimum CRPS estimation. *Mon. Wea. Rev.*, *133*, 1098–1118. doi:
362 10.1175/MWR2904.1
- 363 Huffman, G. J., Bolvin, D. T., Nelkin, E. J., Wolff, D. B., Adler, R. F., Gu, G.,
364 ... Stocker, E. F. (2007). The TRMM multisatellite precipitation analysis
365 (TMPA): Quasi-global, multiyear, combined-sensor precipitation estimates at
366 fine scales. *J. Hydrometeorol.*, *8*(1), 38–55. doi: 10.1175/JHM560.1
- 367 Janicot, S., Caniaux, G., Chauvin, F., de Coëtlogon, G., Fontaine, B., Hall, N., ...
368 Taylor, C. M. (2011). Intraseasonal variability of the West African monsoon.
369 *Atmos. Sci. Lett.*, *12*(1), 58–66. doi: 10.1002/asl.280
- 370 Knippertz, P., Fink, A., Deroubaix, A., Morris, E., Tocquer, F., Evans, M., ...
371 Schlueter, A. (2017). A meteorological and chemical overview of the DAC-
372 CIWA field campaign in West Africa in June–July 2016. *Atmos. Chem. Phys.*,
373 *17*, 10893–10918. doi: 10.5194/acp-17-10893-2017
- 374 Lavaysse, C., Diedhiou, A., Laurent, H., & Lebel, T. (2006). African easterly waves
375 and convective activity in wet and dry sequences of the West African monsoon.
376 *Climate Dyn.*, *27*, 319–332. doi: 10.1007/s00382-006-0137-5
- 377 Maranan, M., Fink, A. H., & Knippertz, P. (2018). Rainfall types over southern
378 West Africa: Objective identification, climatology and synoptic environment.
379 *Quart. J. Roy. Meteorol. Soc.*, *144*, 1628–1648. doi: 10.1002/qj.3345
- 380 Marsham, J. H., Dixon, N. S., Garcia-Carreras, L., Lister, G. M. S., Parker,
381 D. J., Knippertz, P., & Birch, C. E. (2013). The role of moist convec-
382 tion in the West African monsoon system – Insights from continental-scale
383 convection-permitting simulations. *Geophys. Res. Lett.*, *40*, 1843–1849. doi:
384 10.1002/grl.50347
- 385 Mathon, V., Laurent, H., & Lebel, T. (2002). Mesoscale convective system rainfall
386 in the Sahel. *J. Appl. Meteorol.*, *41*, 1081–1092. doi: 10.1175/1520-0450(2002)
387 041<1081:MCSRIT>2.0.CO;2
- 388 Mekonnen, A., Thorncroft, C. D., & Ayyer, A. R. (2006). Analysis of convection
389 and its association with African easterly waves. *J. Climate*, *19*, 5405–5421.
390 doi: 10.1175/JCLI3920.1
- 391 Nesbitt, S. W., Cifelli, R., & Rutledge, S. A. (2006). Storm morphology and rainfall
392 characteristics of TRMM precipitation features. *Mon. Wea. Rev.*, *134*, 2702–
393 2721. doi: 10.1175/MWR3200.1
- 394 Nicholson, S. E. (2008). The intensity, location and structure of the tropical rainbelt
395 over west Africa as factors in interannual variability. *Int. J. Climatol.*, *28*(13),
396 1775–1785. doi: 10.1002/joc.1507
- 397 Pante, G., & Knippertz, P. (2019). Resolving Sahelian thunderstorms improves mid-
398 latitude weather forecasts. *Nature Comm.*, *10*(1), 3487. doi: 10.1038/s41467-
399 -019-11081-4
- 400 Raftery, A. E., Gneiting, T., Balabdaoui, F., & Polakowski, M. (2005). Using
401 Bayesian model averaging to calibrate forecast ensembles. *Mon. Wea. Rev.*,
402 *133*, 1155–1174. doi: 10.1175/MWR2906.1
- 403 Reed, R. J., Norquist, D. C., & Recker, E. E. (1977). The structure and proper-
404 ties of African wave disturbances as observed during phase III of GATE. *Mon.*
405 *Wea. Rev.*, *105*, 317–333. doi: 10.1175/1520-0493(1977)105,0317:TSAPOA.2.0
406 .CO;2
- 407 Roca, R., Aublanc, J., Chambon, P., Fiolleau, T., & Viltard, N. (2014). Ro-
408 bust observational quantification of the contribution of mesoscale convec-
409 tive systems to rainfall in the tropics. *J. Climate*, *27*(13), 4952–4958. doi:
410 10.1175/JCLI-D-13-00628.1
- 411 Roehrig, R., Chauvin, F., & Lafore, J.-P. (2011). 10–25 day intraseasonal variability
412 of convection over the Sahel: a role of the Saharan heat low and midlatitudes.
413 *J. Climate*, *24*, 5863–5878. doi: 10.1175/2011JCLI3960.1
- 414 Scheuerer, M. (2014). Probabilistic quantitative precipitation forecasting using en-
415 semble model output statistics. *Quart. J. Roy. Meteorol. Soc.*, *140*, 1086–1096.

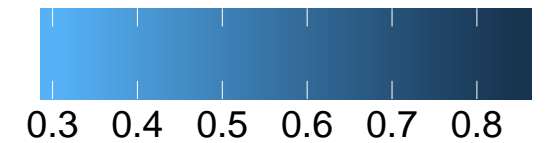
- 416 doi: 10.1002/qj.2183
- 417 Schlueter, A., Fink, A. H., & Knippertz, P. (2019). A systematic comparison of
- 418 tropical waves over northern Africa. Part II: Dynamics and thermodynamics.
- 419 *J. Climate*, *32*, 2605–2625. doi: 10.1175/JCLI-D-18-0651.1
- 420 Schlueter, A., Fink, A. H., Knippertz, P., & Vogel, P. (2019). A systematic compar-
- 421 ison of tropical waves over northern Africa. Part I: Influence on rainfall. *J. Cli-*
- 422 *mate*, *32*, 1501–1523. doi: 10.1175/JCLI-D-18-0173.1
- 423 Schove, D. J. (1946). Note on equatorial forecasting technique. *Quart. J. Roy. Mete-*
- 424 *orol. Soc.*, *72*, 110–112.
- 425 Singh, C., Daron, J., Bazaz, A., Ziervogel, G., Spear, D., Krishnaswamy, J., ...
- 426 Kituyi, E. (2018). The utility of weather and climate information for adap-
- 427 tation decision-making: current uses and future prospects in Africa and India.
- 428 *Climate Develop.*, *10*(5), 389–405. doi: 10.1080/17565529.2017.1318744
- 429 Sloughter, J. M., Raftery, A. E., Gneiting, T., & Fraley, C. (2007). Probabilistic
- 430 quantitative precipitation forecasting using Bayesian model averaging. *Mon.*
- 431 *Wea. Rev.*, *135*, 3209–3220. doi: 10.1175/MWR3441.1
- 432 Vizu, E. K., & Cook, K. H. (2014). Impact of cold air surges on rainfall variability
- 433 in the Sahel and wet African tropics: a multi-scale analysis. *Clim. Dyn.*, *43*,
- 434 1057–1081. doi: 10.1007/s00382-013-1953-z
- 435 Vogel, P., Knippertz, P., Fink, A. H., Schlueter, A., & Gneiting, T. (2018).
- 436 Skill of global raw and postprocessed ensemble, predictions of rainfall over
- 437 northern tropical Africa. *Wea. Forecasting*, *33*, 369–388. doi: 10.1175/
- 438 WAF-D-17-0127.1
- 439 Wani, S., Sreedevi, T., Rockström, J., & Ramakrishna, Y. (2009). Rainfed agricul-
- 440 ture – Past trends and future prospects. In S. Wani, J. Rockström, & T. Oweis
- 441 (Eds.), *Rainfed agriculture: Unlocking the potential* (Vol. 7, pp. 1–35). Walling-
- 442 ford, UK.
- 443 Wilks, D. S. (2019). *Statistical methods in the atmospheric sciences* (4th ed.). Ams-
- 444 terdam: Elsevier.

Figure 1.

Lag 1



Probability of precipitation



Lag 2

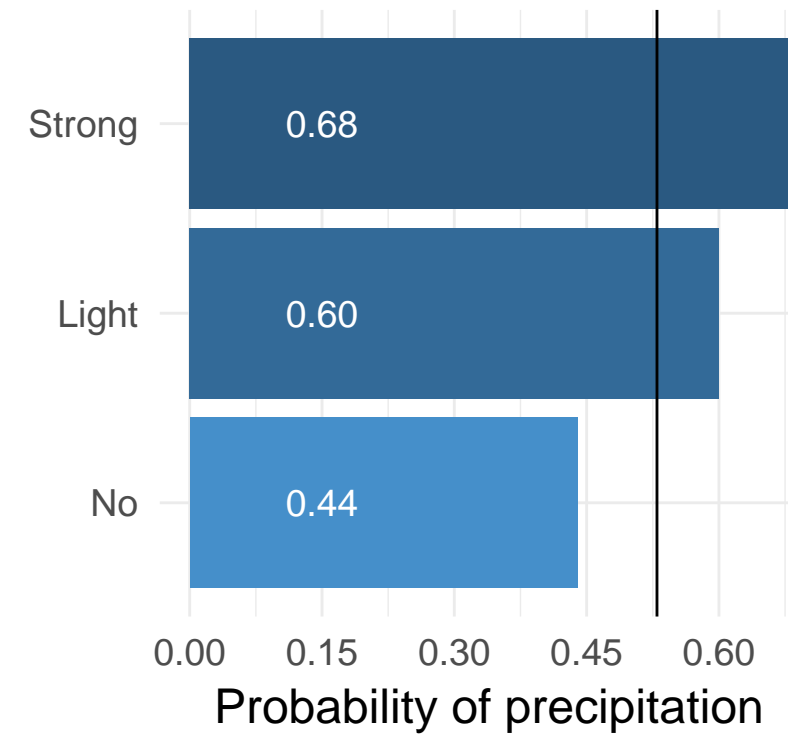
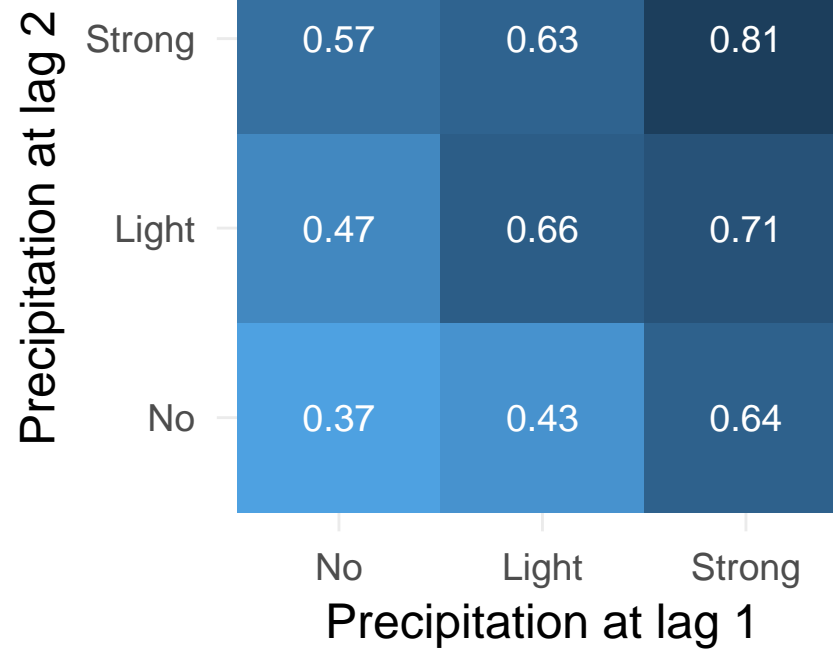
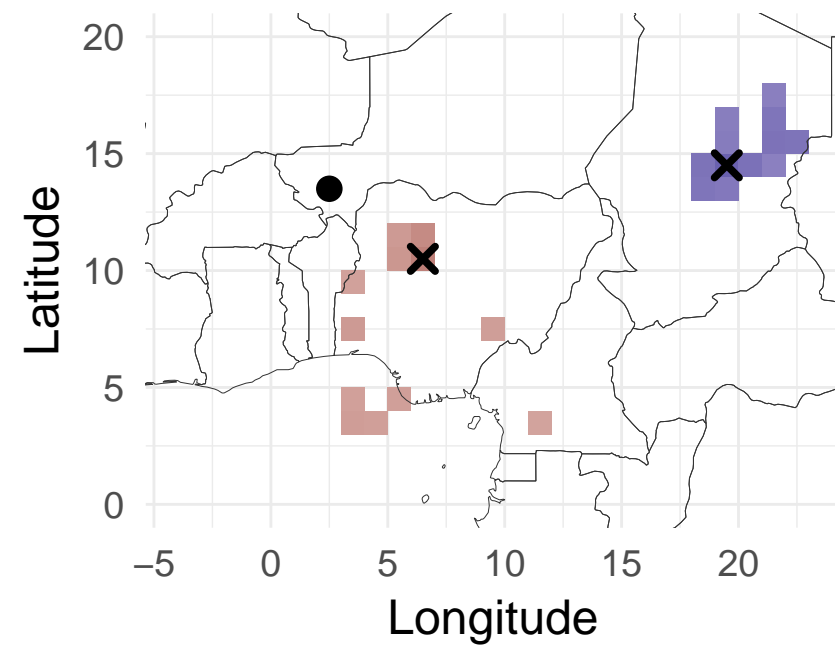


Figure 2.

Niamey (Niger) July – September 2016

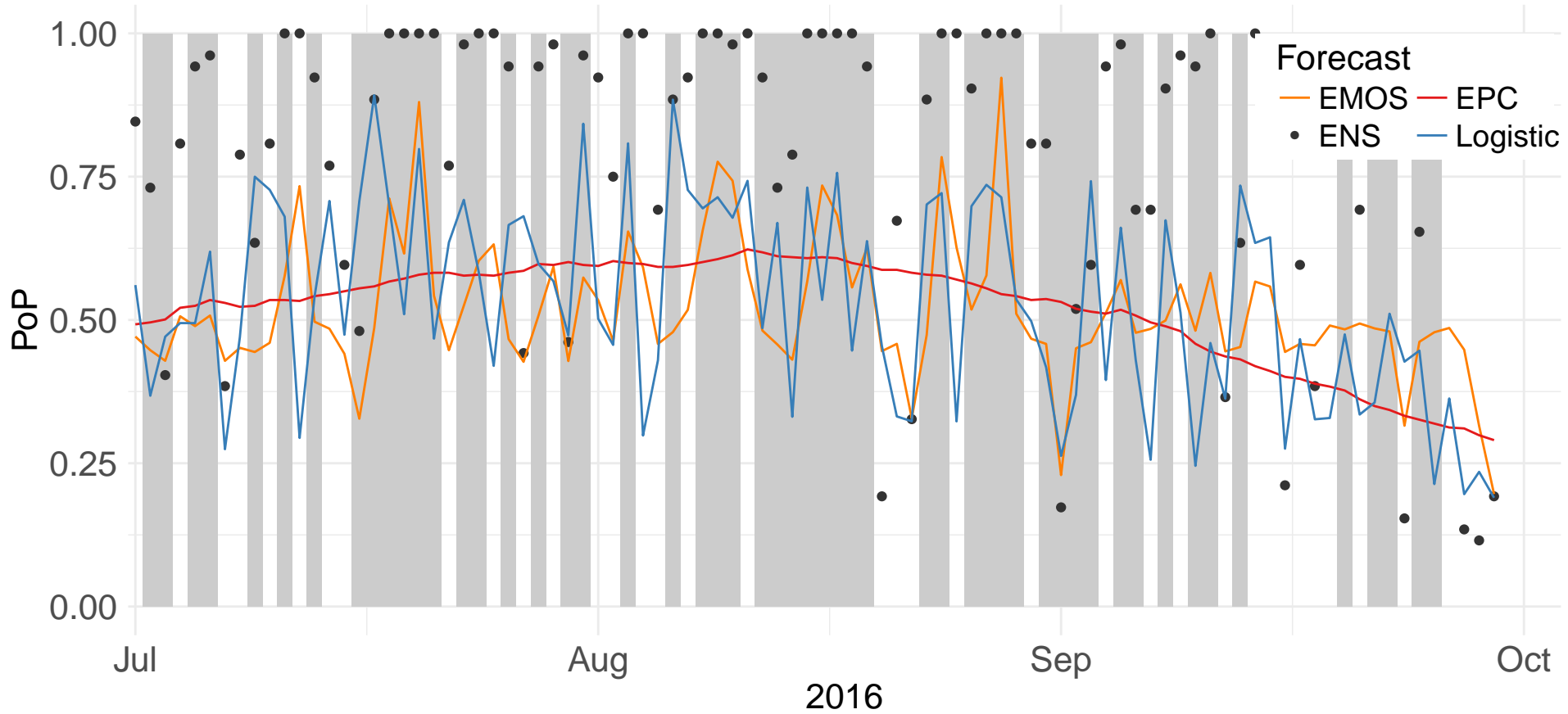
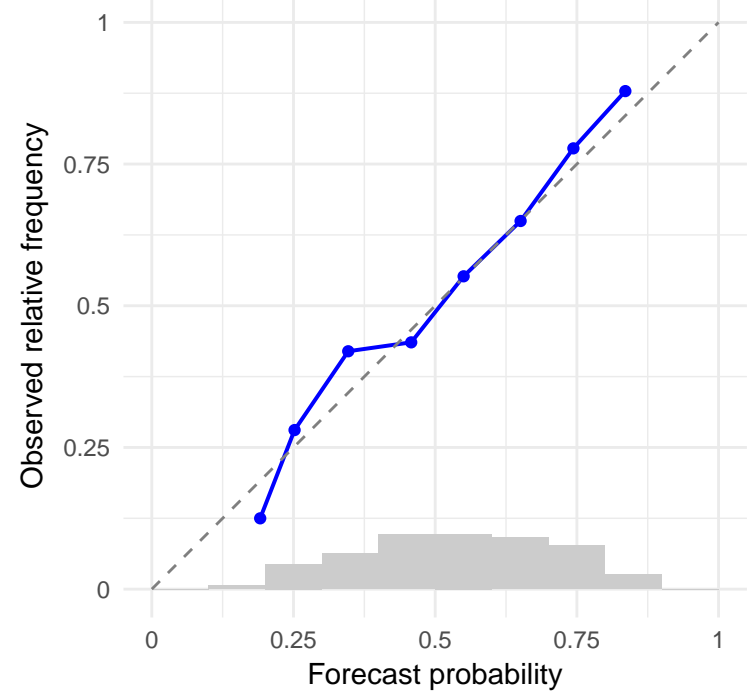
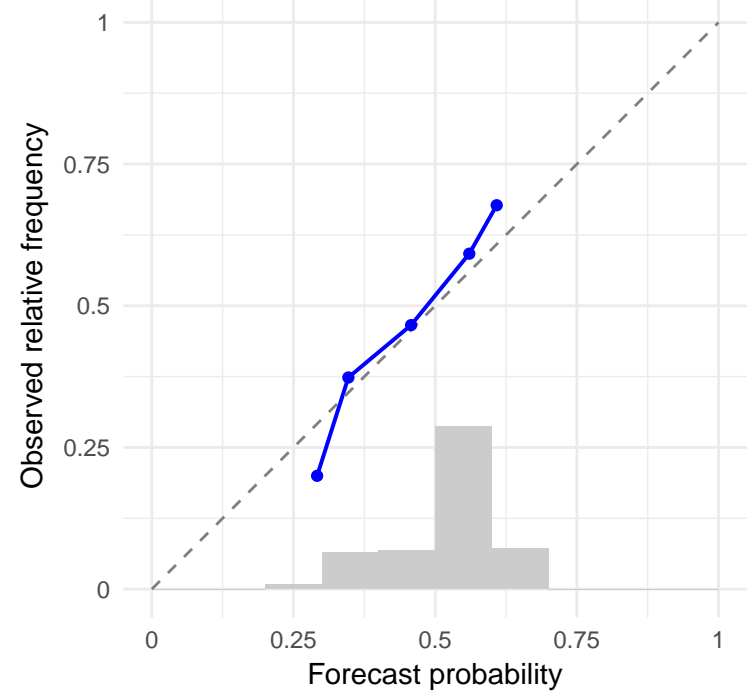


Figure 3.

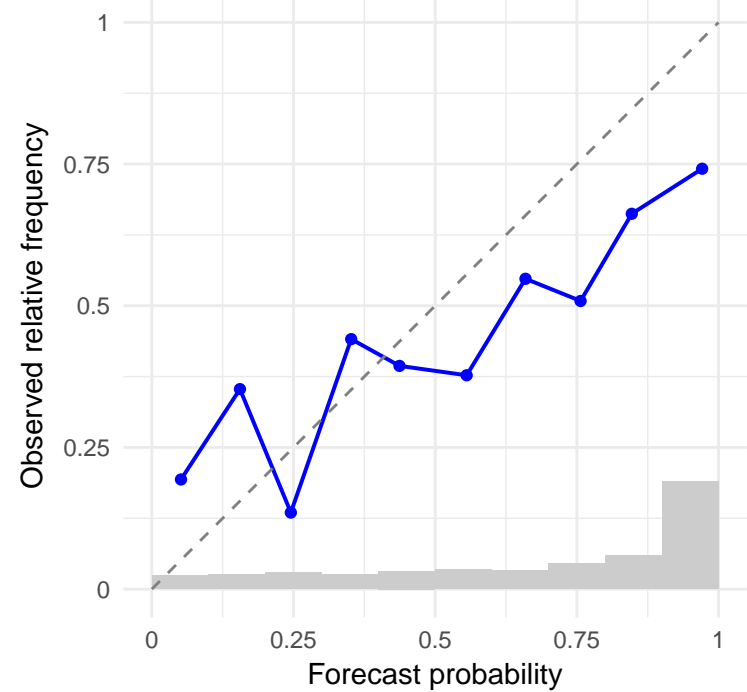
a) Logistic



b) EPC



c) ENS



d) EMOS

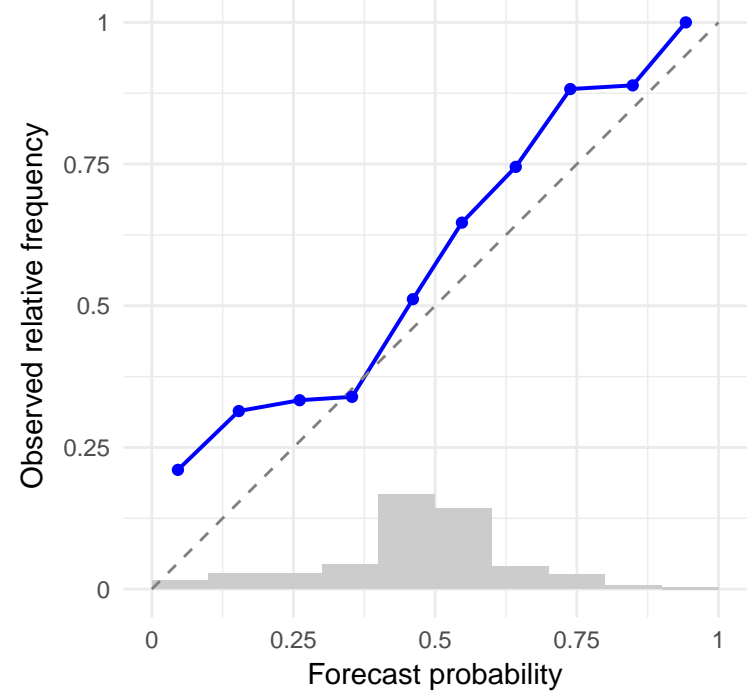
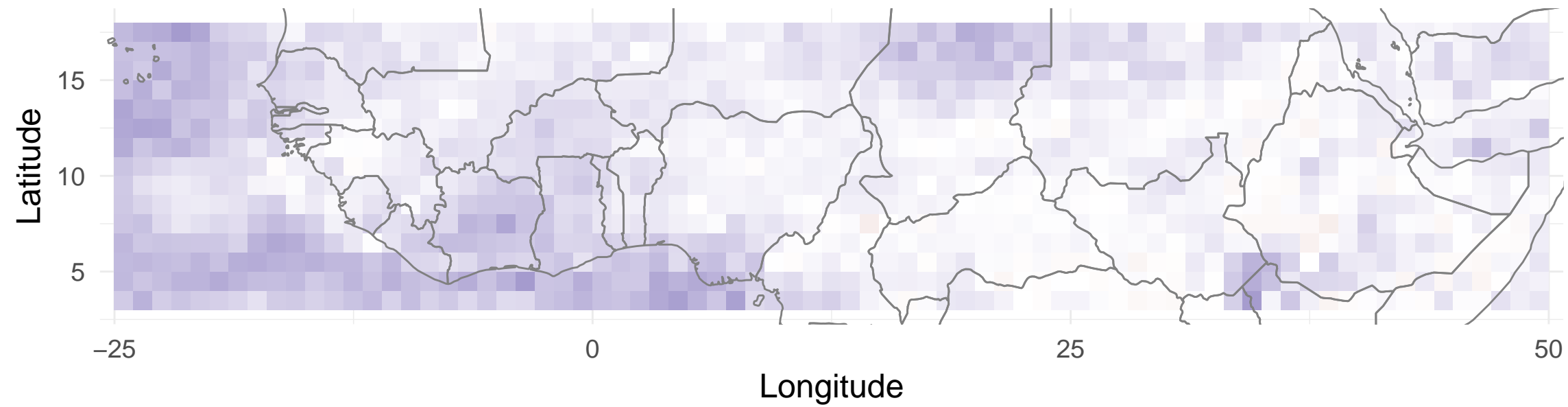


Figure 4.

a) Logistic vs. EPC



b) Logistic vs. EMOS

